

Rabi splitting of the optical intersubband absorption line of multiple quantum wells inside a Fabry-Pérot microcavity

Ansheng Liu

Institute of Physics, Aalborg University, Pontoppidanstræde 103, DK-9220 Aalborg Øst, Denmark

(Received 1 May 1996; revised manuscript received 3 September 1996)

In a nonlocal semiclassical local-field approach and by using a simple one-band model in which the conduction-band nonparabolicity is taken into account in an energy-dependent effective-mass scheme, we have derived a rigorous expression for the p -polarized optical intersubband absorption coefficient of a multiple-quantum-well (MQW) structure inside an asymmetric Fabry-Pérot microcavity. For a GaAs/Al_xGa_{1-x}As MQW structure sandwiched between a GaAs/AlAs distributed Bragg reflector and vacuum, we performed numerical calculations of the optical-absorption spectra for different parameters such as the cavity length, the angle of incidence, the electron concentration, and the number of quantum wells (QW's) in the structure. In the strong-coupling regime, our results show that the so-called Rabi splitting of the absorption spectrum, which is due to the electromagnetic interactions between the cavity modes and the intersubband modes, is increased in size with an increase in the QW number and in the sheet electron density. The contrast of the splitting is also found to be strongly dependent of these parameters. Finally, it is demonstrated that the Rabi splitting of the intersubband absorption line can be easily tuned by varying either the cavity length or the angle of incidence. [S0163-1829(97)07111-7]

I. INTRODUCTION

Since the experimental observation of the optical intersubband transition in semiconductor quantum well (QW) systems by West and Eglash,¹ the linear optical absorption of a multiple-quantum-well (MQW) structure has been extensively studied.²⁻⁶ The main attention of the previous work was devoted to a fundamental understanding of the many-body effect and the dynamic screening in quasi-two-dimensional systems.⁴⁻¹⁰ Recently there were a number of publications dealing with the radiative electromagnetic interactions of QW's in conjunction with both intersubband¹¹ and interband (excitonic) transitions.¹²⁻¹⁴ By use of a nonlocal optical conductivity or susceptibility describing the electromagnetic response of the QW system, it has been shown that the QW optical spectra can be significantly modified by varying the QW number¹¹ and the QW separation (the barrier thickness) in the structure.¹⁴ In a more recent paper,¹⁵ the present author also showed that the electromagnetic interaction among QW's can be enhanced through the light total reflection from a barrier material-vacuum interface. As a result, the optical intersubband absorption spectra of the MQW structure are significantly changed by an inclusion of the barrier-vacuum boundary.¹⁵ On the basis of these studies, one would expect that the optical properties of MQW's should also be modified with the presence of a microcavity. Indeed, it has been shown both theoretically and experimentally that the absorptive and radiative properties of excitons in semiconductor QW's embedded in a microcavity can be substantially different from those of the free-standing QW's.¹⁶⁻²³ In particular, it has been experimentally demonstrated that, due to the electromagnetic coupling between cavity modes and excitons, the so-called normal-mode or vacuum-field Rabi splitting of the excitonic transmission-absorption spectrum can occur.^{17,20,23} In contrast, the micro-

cavity effect on the intersubband absorption line has only been investigated theoretically and unsystematically. In the early work of Dahl and Sham,²⁴ the coupling of the intersubband modes and cavity modes was partially discussed in the context of the electromagnetic properties of the quasi-two-dimensional electrons in inversion layers in metal-oxide-semiconductor junctions. Neglecting the line broadening effect, which is unavoidable for actual samples, the authors demonstrated the existence of the splitting of the intersubband modes and the cavity modes. However, the size of such splitting was estimated to be very small, and typically much less than the width of the intersubband resonance.²⁴ Therefore, it seems impossible to experimentally observe such splitting in the electron systems treated in that paper.²⁴ Quite recently, the present author suggested that the Rabi splitting of the intersubband absorption line of MQW's placed between a dielectric prism and vacuum can be observable, provided that a sufficiently large number of QW's are involved in optical transitions.²⁵ Nevertheless, in that paper,²⁵ the dependence of the size of the Rabi splitting on the cavity and QW parameters was not discussed in detail.

The aim of the present paper is to present a comprehensive investigation of the microcavity effect in the linear optical intersubband response of MQW's inside a Fabry-Pérot microcavity. Our attention is especially focused on the electromagnetic coupling between cavity modes and intersubband modes in the strong-coupling regime. The dependence of the Rabi splitting of the intersubband absorption spectrum on various cavity and QW parameters such as the cavity length, the number of QW's, the electron intersubband relaxation time, and the electron concentration is numerically investigated. Being different from the previous work,^{24,25} the present paper deals with an asymmetric cavity in which one mirror is a *single* distributed Bragg reflector (DBR) and the other is a light-total-reflection dielectric interface.

In Sec. II, we derive a general and rigorous expression for

the optical intersubband absorption coefficient of the MQW-embedded microcavity in a combined transfer-matrix and Green's-function approach. Namely, we use the transfer-matrix method to describe the optical response of the homogeneous multilayers in the DBR, and employ the quasi-vacuum Green's function to analyze the nonlocal response of the electronic intersubband transition in the QW's. The Green's-function formalism has also been adopted previously in the work of Dahl and Sham.²⁴ In their prescription, the defined electromagnetic propagator that describes the propagating properties of light in the whole system in the absence of the electron gas contains two coefficients depending on the particular geometry of the layers. For two semi-infinite media and for a waveguide structure confined by two perfect conductors, the explicit expression for the Green's function was derived.²⁴ However, for the multilayer configuration studied in the present paper, we find our combined transfer-matrix and Green's-function method is more convenient and applicable. In addition, our approach is capable of calculating the optical spectrum of a MQW structure with well and barrier width fluctuations.¹⁵ In Sec. III, we present numerical calculations of the optical absorption spectra of a GaAs/Al_xGa_{1-x}As MQW structure bounded on one side by vacuum and on the other side by a GaAs/AlAs DBR followed by a GaAs prism. The influence of the structure parameters on the absorption spectrum is discussed.

II. THEORY

Consider a MQW structure consisting of N n -type doped quantum wells (not necessarily identical) embedded arbitrarily in a barrier material characterized by a relative dielectric constant $\varepsilon_2(\omega)$. The MQW structure is sandwiched between a semi-infinite medium of a dielectric constant $\varepsilon_3(\omega)$ and a distributed Bragg reflector constructed from N_m periods of two alternating component media having dielectric constants of $\varepsilon_1(\omega)$ and $\varepsilon_4(\omega)$. The thicknesses of media 1 (ε_1) and 4 (ε_4) are L_1 and L_4 , respectively. The spatial period of the DBR is denoted by $L=L_1+L_4$. The last constitutive layer in the DBR is medium 1, which connects with the barrier medium 2 (ε_2). The other side of the DBR is limited by a semi-infinitely extended medium 1 serving as a prism. In a Cartesian xyz coordinate system, it is assumed that the z axis points along the direction normal to the interfaces of the MQW structure, and that the media 1-2 and media 2-3 boundaries are positioned at $z=0$ and $z=\Lambda$, respectively. Furthermore, we assume that the QW's in the MQW structure are well separated in space, and there is no overlap of the envelope functions belonging to different quantum wells. As a result, the subbands of the MQW structure are practically indistinguishable from those of an isolated quantum well. It is also assumed that each QW in the MQW structure has only two bound subbands involved in intersubband transitions within the conduction band. Consequently, light-induced current density in each quantum well can be regarded as being localized within an effective width d_m ($m=1,2,\dots,N$), which is somewhat larger than the thickness of the corresponding well layer. Along the z axis, the effective well layers are positioned at D_m ($m=1,2,\dots,N$) with $D_1=a$ and $D_N=\Lambda-d_N-b$, where a and b denote the thicknesses of barrier layers between the DBR and the first well

layer and between the last well layer and medium 3. Therefore, for a given value of well and barrier widths in the MQW structure, the total length of the microcavity denoted by Λ is determined by the total number of QW's as well as a and b .

Let us now assume that a p -polarized electromagnetic wave of angular frequency ω is incident at an angle θ from the prism onto the MQW structure, and that the scattering plane is placed parallel to the xz plane. Due to the translational invariance of our system parallel to the interfaces (xy plane), all vector field components (F) appearing in the analysis have the general form

$$F(\mathbf{r},t)=F(z)e^{i(q_{\parallel}x-\omega t)}, \quad (1)$$

$q_{\parallel}=(\omega/c_0)\sqrt{\varepsilon_1}\sin\theta$ being the x component of the wave vector of light. Therefore the z -dependent local electric field $\mathbf{E}(z)=[E_x(z),0,E_z(z)]$ satisfies the following wave equation:

$$\vec{\mathcal{L}}\cdot\mathbf{E}(z)=-i\mu_0\omega\mathbf{J}(z). \quad (2)$$

In the above equation, the tensorial operator $\vec{\mathcal{L}}$ is given in dyadic form by

$$\vec{\mathcal{L}}=\vec{\mathbf{U}}\left[\varepsilon(\omega,z)\frac{\omega^2}{c_0^2}-q_{\parallel}^2+\frac{\partial^2}{\partial z^2}\right]-\left(iq_{\parallel}\mathbf{e}_x+\mathbf{e}_z\frac{\partial}{\partial z}\right)\left(iq_{\parallel}\mathbf{e}_x+\mathbf{e}_z\frac{\partial}{\partial z}\right), \quad (3)$$

where $\vec{\mathbf{U}}$ is the unit tensor, and \mathbf{e}_x and \mathbf{e}_z are the unit vectors along the x and z directions, respectively. For the MQW-embedded microcavity structure under consideration, the local, isotropic dielectric constant in the different regions is given by

$$\varepsilon(\omega,z)=\begin{cases} \varepsilon_4(\omega), & (n-1)L < z < (n-1)L+L_4 \\ & (n=-N_m+1,-N_m+2,\dots,0) \\ \varepsilon_2(\omega), & 0 \leq z \leq \Lambda \\ \varepsilon_3(\omega), & z > \Lambda \\ \varepsilon_1(\omega), & \text{otherwise.} \end{cases} \quad (4)$$

Note that, for simplicity, we have ignored the small difference of the background dielectric constants between the barrier and well layers inside the MQW region ($0 < z < \Lambda$). The effect of the dielectric mismatching between constituent semiconductors on the collective intrasubband and intersubband excitation of a single QW structure was previously considered by Wendler and Kändler.²⁶ On the right-hand side of Eq. (2), $\mathbf{J}(z)$ is the light-induced current density associated with the intersubband transition of QW's. On the basis of the above-mentioned assumption, $\mathbf{J}(z)=0$ when z is outside the effective well layers, and

$$\mathbf{J}(z)=\int_{D_m}^{D_m+d_m}\vec{\sigma}^{(m)}(z,z')\cdot\mathbf{E}(z')dz' \quad (5)$$

for $D_m < z, z' < D_m+d_m$. In Eq. (5), the tensor $\vec{\sigma}^{(m)}(z,z')$ is the paramagnetic (current-current correlated) part of the linear nonlocal conductivity response function of the m th quan-

tum well. Since only the z component of the local electric field induces an electric-dipole-allowed intersubband transition, it is a good approximation to neglect the xx component of the nonlocal conductivity tensor of QW's in our analysis. In a simple one-band scheme, and within the framework of the random-phase approximation, the relevant nonzero element of the nonlocal conductivity tensor is given, in the so-called long-wavelength ($q_{\parallel} \rightarrow 0$) and low-temperature ($T \rightarrow 0$) limits, by²⁷⁻²⁹

$$\sigma_{zz}^{(m)}(z, z') = \frac{ie^2}{4\pi\omega(m^*)^2} \frac{m_{\parallel 1}^{*(m)} m_{\parallel 2}^{*(m)}}{m_{\parallel 1}^{*(m)} - m_{\parallel 2}^{*(m)}} \Phi^{(m)}(z) \Phi^{(m)}(z') \times \ln \left(\frac{[\hbar(\omega + i/\tau)]^2 - [E_2^{(m)} - E_1^{(m)}]^2}{[\hbar(\omega + i/\tau)]^2 - [E_2^{(m)} - E_1^{(m)} + \Delta E^{(m)}]^2} \right), \quad (6)$$

$$\Delta E^{(m)} = \left(\frac{m_{\parallel 1}^{*(m)}}{m_{\parallel 2}^{*(m)}} - 1 \right) [E_F^{(m)} - E_1^{(m)}], \quad (7)$$

with

$$\Phi^{(m)}(z) = \psi_1^{(m)}(z) \frac{d\psi_2^{(m)}(z)}{dz} - \psi_2^{(m)}(z) \frac{d\psi_1^{(m)}(z)}{dz}. \quad (8)$$

In Eq. (6) m^* is the effective mass of electrons, τ is a phenomenological relaxation time in connection with intersubband transitions, and finally $m_{\parallel j}^{*(m)}$ ($j=1,2$) is the so-called parallel effective mass of the m th quantum well, which originates in the conduction-band nonparabolicity effect.³⁰ In the present paper the nonparabolicity effect was taken into account in the energy-dependent effective-mass scheme proposed by Ekenberg.³⁰ Thus the anisotropy of the conduction band has been included. The quantity $E_F^{(m)}$ appearing in Eq. (7) is the Fermi energy of m th quantum well, which is determined from the surface electron density in the well. Note that, in our theory, τ is only due to ‘‘pure dephasing’’ processes such as scattering with other quasiparticles, which leads to a homogeneous line broadening. In addition, the band nonparabolicity contribution to the line broadening is also incorporated through Eqs. (6) and (7). The single-particle envelope wave functions $[\psi_1^{(m)}(z)$ and $\psi_2^{(m)}(z)$, $m=1,2,\dots,N$] and the corresponding energy eigenvalues ($E_1^{(m)}$ and $E_2^{(m)}$, $m=1,2,\dots,N$) are calculated self-consistently by solving the coupled one-band effective-mass Schrödinger equation and Poisson equation,³¹ with taking into account the exchange and correlation effects in the local-density approximation.

Recalling the fact that the current density $\mathbf{J}(z)$ vanishes outside the effective well layers, it is straightforward to solve Eq. (2) in the regions of $z < 0$ and $z > \Lambda$. The electric field distribution with each homogeneous layer inside these regions (including layers in the DBR) can be expressed as a sum of a forward-propagating plane wave and a backward-propagating plane wave. Denoting the x components of the incident and reflected amplitudes of the electric field in the prism ($z < -N_m L$) by A_0 and B_0 , and following the transfer-matrix method of Yeh, Yariv, and Hong,³² we find the x components of the forward (A_1) and backward (B_1)

amplitudes in the last layer of the DBR ($-L_1 < z < 0$) are determined from the matrix equation

$$\begin{pmatrix} A_0 \\ B_0 \end{pmatrix} = \begin{pmatrix} T_{11} & T_{12} \\ T_{21} & T_{22} \end{pmatrix}^{N_m} \begin{pmatrix} A_1 \\ B_1 \end{pmatrix} \equiv \vec{\mathbf{T}} \begin{pmatrix} A_1 \\ B_1 \end{pmatrix}. \quad (9)$$

Here, the 2×2 matrix $\vec{\mathbf{T}}$ is called the transfer matrix. For p -polarized light, the matrix elements are³²

$$T_{11} = e^{-iq_{\perp 1} L_1} \left[\cos(q_{\perp 4} L_4) - \frac{i}{2} \left(\frac{\varepsilon_4 q_{\perp 1}}{\varepsilon_1 q_{\perp 4}} + \frac{\varepsilon_1 q_{\perp 4}}{\varepsilon_4 q_{\perp 1}} \right) \sin(q_{\perp 4} L_4) \right], \quad (10)$$

$$T_{12} = e^{iq_{\perp 1} L_1} \left[-\frac{i}{2} \left(\frac{\varepsilon_4 q_{\perp 1}}{\varepsilon_1 q_{\perp 4}} - \frac{\varepsilon_1 q_{\perp 4}}{\varepsilon_4 q_{\perp 1}} \right) \sin(q_{\perp 4} L_4) \right], \quad (11)$$

$$T_{21} = e^{-iq_{\perp 1} L_1} \left[\frac{i}{2} \left(\frac{\varepsilon_4 q_{\perp 1}}{\varepsilon_1 q_{\perp 4}} - \frac{\varepsilon_1 q_{\perp 4}}{\varepsilon_4 q_{\perp 1}} \right) \sin(q_{\perp 4} L_4) \right], \quad (12)$$

$$T_{22} = e^{iq_{\perp 1} L_1} \left[\cos(q_{\perp 4} L_4) + \frac{i}{2} \left(\frac{\varepsilon_4 q_{\perp 1}}{\varepsilon_1 q_{\perp 4}} + \frac{\varepsilon_1 q_{\perp 4}}{\varepsilon_4 q_{\perp 1}} \right) \sin(q_{\perp 4} L_4) \right], \quad (13)$$

$$q_{\perp i} = \left[\frac{\omega^2}{c_0^2} \varepsilon_i(\omega) - q_{\parallel}^2 \right]^{1/2}, \quad i=1,2,3,4, \quad (14)$$

being the perpendicular (z) component of the wave vector of the plane wave in medium i . In the region of $-L_1 < z < 0$, the electric field can be written as

$$\mathbf{E}(z) = (A_1 e^{iq_{\perp 1} z} + B_1 e^{-iq_{\perp 1} z}) \mathbf{e}_x - \frac{q_{\parallel}}{q_{\perp 1}} (A_1 e^{iq_{\perp 1} z} - B_1 e^{-iq_{\perp 1} z}) \mathbf{e}_z. \quad (15)$$

Inside medium 3 ($z > \Lambda$), because there exists no backward-propagating wave, the electric field takes the form

$$\mathbf{E}(z) = A_3 e^{iq_{\perp 3} z} \mathbf{e}_x - \frac{q_{\parallel}}{q_{\perp 3}} A_3 e^{iq_{\perp 3} z} \mathbf{e}_z, \quad (16)$$

where A_3 is the x component of the amplitude of the transmitted field.

In the region $0 \leq z \leq \Lambda$ the solution of the wave equation is more complicated because of the existence of the light-induced current density. In the electromagnetic scattering formalism, a formal solution of the wave equation can be written as¹¹

$$\mathbf{E}(z) = \mathbf{E}^B(z) - i\mu_0\omega \sum_{m=1}^N \int_{D_m} \int_{D_m}^{D_m+d_m} \vec{\mathbf{G}}(z, z') \cdot \vec{\mathbf{G}}^{(m)}(z', z'') \cdot \mathbf{E}(z'') dz'' dz', \quad (17)$$

where

$$\mathbf{E}^B(z) = (A_2 e^{iq_{\perp 2} z} + B_2 e^{-iq_{\perp 2} z}) \mathbf{e}_x - \frac{q_{\parallel}}{q_{\perp 2}} (A_2 e^{iq_{\perp 2} z} - B_2 e^{-iq_{\perp 2} z}) \mathbf{e}_z \quad (18)$$

is the so-called background field with two so-far-undetermined constants A_2 and B_2 . The background field satisfies the homogeneous part of Eq. (2). The second term on the right-hand side of Eq. (17) is regarded as a particular solution of Eq. (2). Note that in this paper we have used the convention that the imaginary part of the z component of the wave vector, i.e., $q_{\perp i}$ ($i=2,3,4$) is positive if it is complex ($q_{\perp 1}$ is assumed to be real). The tensor $\mathbf{G}(z, z')$ entering Eq. (17) is the quasivacuum electromagnetic propagator (Green's function), which is defined via

$$\vec{\mathcal{L}}' \cdot \vec{\mathbf{G}}(z, z') = \vec{\mathbf{U}} \delta(z - z'), \quad (19)$$

where δ is the Dirac delta function, and $\vec{\mathcal{L}}'$ is obtained from Eq. (3) by letting $\varepsilon(\omega, z) = \varepsilon_2(\omega)$. The Green's function has been derived by a number of authors, and the relevant components are given by^{26,33}

$$G_{xz}(z, z') = \frac{q_{\parallel}}{2i\varepsilon_2} \left(\frac{c_0}{\omega} \right)^2 \text{sgn}(z' - z) \exp(iq_{\perp 2} |z - z'|), \quad (20)$$

$$G_{zz}(z, z') = \frac{q_{\parallel}^2}{2i\varepsilon_2 q_{\perp 2}} \left(\frac{c_0}{\omega} \right)^2 \exp(iq_{\perp 2} |z - z'|) + \left(\frac{c_0}{\omega} \right)^2 \frac{1}{\varepsilon_2} \delta(z - z'), \quad (21)$$

where $\text{sgn}(x)$ is the usual sign function, i.e., $\text{sgn}(x) = 1$ for $x > 0$ and $\text{sgn}(x) = -1$ for $x < 0$.

Inserting Eq. (6) into Eq. (17), one obtains, for $0 \leq z \leq \Lambda$,

$$E_x(z) = E_x^B(z) + \sum_{m=1}^N \alpha^{(m)}(\omega) F_{xz}^{(m)}(z) \beta^{(m)}, \quad (22)$$

$$E_z(z) = E_z^B(z) + \sum_{m=1}^N \alpha^{(m)}(\omega) F_{zz}^{(m)}(z) \beta^{(m)}, \quad (23)$$

where

$$\alpha^{(m)}(\omega) = \frac{\mu_0 e^2}{4\pi(m^*)^2} \frac{m_{\parallel 1}^{*(m)} m_{\parallel 2}^{*(m)}}{m_{\parallel 1}^{*(m)} - m_{\parallel 2}^{*(m)}} \times \ln \left(\frac{[\hbar(\omega + i/\tau)]^2 - [E_2^{(m)} - E_1^{(m)}]^2}{[\hbar(\omega + i/\tau)]^2 - [E_2^{(m)} - E_1^{(m)} + \Delta E^{(m)}]^2} \right), \quad (24)$$

$$F_{xz}^{(m)}(z) = \int_{D_m}^{D_m+d_m} G_{xz}(z, z') \Phi^{(m)}(z') dz', \quad (25)$$

and

$$F_{zz}^{(m)}(z) = \int_{D_m}^{D_m+d_m} G_{zz}(z, z') \Phi^{(m)}(z') dz'. \quad (26)$$

As a definition, the quantities $\beta^{(m)}$ ($m=1, 2, \dots, N$) are related to the local field by

$$\beta^{(m)} = \int_{D_m}^{D_m+d_m} E_z(z'') \Phi^{(m)}(z'') dz''. \quad (27)$$

For nonmagnetic materials studied in this paper, the displacement field vector is related to the electric field via

$$\mathbf{D}(z) = \varepsilon_0 \int \left[\varepsilon(\omega, z) \vec{\mathbf{U}} \delta(z - z') + \frac{i \vec{\sigma}(z, z')}{\varepsilon_0 \omega} \right] \cdot \mathbf{E}(z') dz'. \quad (28)$$

By combining Eqs. (15) and (16) with Eqs. (22) and (23), and by using the usual electromagnetic boundary conditions, i.e., continuities of E_x and D_z across the interfaces at $z=0$ and Λ , one obtains the following linear equations:

$$A_1 + B_1 = A_2 + B_2 + \sum_{m=1}^N \alpha^{(m)} F_{xz}^{(m)}(0) \beta^{(m)}, \quad (29)$$

$$A_1 - B_1 = \frac{\varepsilon_2 q_{\perp 1}}{\varepsilon_1 q_{\perp 2}} (A_2 - B_2) - \frac{\varepsilon_2 q_{\perp 1}}{\varepsilon_1 q_{\parallel}} \sum_{m=1}^N \alpha^{(m)} F_{zz}^{(m)}(0) \beta^{(m)}, \quad (30)$$

$$A_3 e^{iq_{\perp 3} \Lambda} = A_2 e^{iq_{\perp 2} \Lambda} + B_2 e^{-iq_{\perp 2} \Lambda} + \sum_{m=1}^N \alpha^{(m)} F_{xz}^{(m)}(\Lambda) \beta^{(m)}, \quad (31)$$

$$A_3 e^{iq_{\perp 3} \Lambda} = \frac{\varepsilon_2 q_{\perp 3}}{\varepsilon_3 q_{\perp 2}} (A_2 e^{iq_{\perp 2} \Lambda} - B_2 e^{-iq_{\perp 2} \Lambda}) - \frac{\varepsilon_2 q_{\perp 3}}{\varepsilon_3 q_{\parallel}} \sum_{m=1}^N \alpha^{(m)} F_{zz}^{(m)}(\Lambda) \beta^{(m)}, \quad (32)$$

where

$$F_{zz}^{(m)}(0) = \frac{q_{\parallel}}{q_{\perp 2}} F_{xz}^{(m)}(0) = \left(\frac{c_0}{\omega} \right)^2 \frac{q_{\parallel}^2}{2i\varepsilon_2 q_{\perp 2}} \int_{D_m}^{D_m+d_m} e^{iq_{\perp 2} z'} \Phi^{(m)}(z') dz', \quad (33)$$

and

$$F_{zz}^{(m)}(\Lambda) = -\frac{q_{\parallel}}{q_{\perp 2}} F_{xz}^{(m)}(\Lambda) = \left(\frac{c_0}{\omega} \right)^2 \frac{q_{\parallel}^2}{2i\varepsilon_2 q_{\perp 2}} e^{iq_{\perp 2} \Lambda} \int_{D_m}^{D_m+d_m} e^{-iq_{\perp 2} z'} \times \Phi^{(m)}(z') dz'. \quad (34)$$

Substituting Eq. (23) into Eq. (27), one realizes that the N unknowns $\beta^{(m)}$ ($m=1, 2, \dots, N$) are determined from the following N linear equations

$$\beta^{(n)} - \sum_{m=1}^N K^{(n,m)} \alpha^{(m)} \beta^{(m)} = -\frac{q_{\parallel}}{q_{\perp 2}} [A_2 S_+^{(n)} - B_2 S_-^{(n)}], \quad (35)$$

where

$$K^{(n,m)} = \int_{D_n}^{D_n+d_n} \Phi^{(n)}(z) F_{zz}^{(m)}(z) dz \quad (36)$$

and

$$S_{\pm}^{(n)} = \int_{D_n}^{D_n+d_n} \Phi^{(n)}(z) e^{\pm i q_{\perp 2} z} dz. \quad (37)$$

By combining Eqs. (29)–(32) with Eq. (35) and eliminating B_1 , A_2 , B_2 , and A_3 , one arrives at

$$\begin{aligned} \beta^{(n)} - \sum_{m=1}^N K^{(n,m)} \alpha^{(m)} \beta^{(m)} + U^{(n)} \sum_{m=1}^N \alpha^{(m)} \beta^{(m)} F_{zz}^{(m)}(0) \\ + V^{(n)} \sum_{m=1}^N \alpha^{(m)} \beta^{(m)} F_{zz}^{(m)}(\Lambda) = W^{(n)} A_1, \end{aligned} \quad (38)$$

where

$$U^{(n)} = \frac{r_{12}}{1 + r_{12} r_{23} \exp(2i q_{\perp 2} \Lambda)} \times [S_+^{(n)} + r_{23} \exp(2i q_{\perp 2} \Lambda) S_-^{(n)}], \quad (39)$$

$$V^{(n)} = \frac{r_{23} \exp(i q_{\perp 2} \Lambda)}{1 + r_{12} r_{23} \exp(2i q_{\perp 2} \Lambda)} [r_{12} S_+^{(n)} - S_-^{(n)}], \quad (40)$$

$$W^{(n)} = -\frac{q_{\parallel}}{q_{\perp 2}} \frac{1 - r_{12}}{1 + r_{12} r_{23} \exp(2i q_{\perp 2} \Lambda)} \times [S_+^{(n)} + r_{23} \exp(2i q_{\perp 2} \Lambda) S_-^{(n)}], \quad (41)$$

with

$$r_{ij} = \frac{q_{\perp i} \varepsilon_j(\omega) - q_{\perp j} \varepsilon_i(\omega)}{q_{\perp i} \varepsilon_j(\omega) + q_{\perp j} \varepsilon_i(\omega)}, \quad i = 1, 2; \quad j = 2, 3 \quad (42)$$

being the well-known p -polarized Fresnel's amplitude reflection coefficient between medium i and medium j . If we regard A_1 as a known quantity, $\beta^{(m)}$ can be solved from Eq. (38). In turn, other unknowns including B_1 and A_3 are also determined. Combining Eqs. (29)–(32), we obtain

$$r_p \equiv -\frac{B_1}{A_1} = r_p^0 - \frac{q_{\perp 2}}{q_{\parallel}} \frac{1 + r_{12}}{1 + r_{12} r_{23} \exp(2i q_{\perp 2} \Lambda)} \sum_{m=1}^N \alpha^{(m)} \tilde{\beta}^{(m)} F_{zz}^{(m)}(0) - \frac{q_{\perp 2}}{q_{\parallel}} \frac{(1 + r_{12}) r_{23} \exp(i q_{\perp 2} \Lambda)}{1 + r_{12} r_{23} \exp(2i q_{\perp 2} \Lambda)} \sum_{m=1}^N \alpha^{(m)} \tilde{\beta}^{(m)} F_{zz}^{(m)}(\Lambda), \quad (43)$$

$$\begin{aligned} t_p \equiv \frac{A_3}{A_1} = t_p^0 + \frac{(1 - r_{23}) \exp(-i q_{\perp 3} \Lambda)}{1 + r_{12} r_{23} \exp(2i q_{\perp 2} \Lambda)} \left\{ \frac{q_{\perp 2}}{q_{\parallel}} r_{12} \exp(i q_{\perp 2} \Lambda) \sum_{m=1}^N \alpha^{(m)} \tilde{\beta}^{(m)} F_{zz}^{(m)}(0) \right. \\ \left. + \left[\left(\frac{q_{\perp 2}}{q_{\parallel}} - 1 \right) r_{12} r_{23} \exp(2i q_{\perp 2} \Lambda) - 1 \right] \sum_{m=1}^N \alpha^{(m)} \tilde{\beta}^{(m)} F_{zz}^{(m)}(\Lambda) \right\}, \end{aligned} \quad (44)$$

where

$$r_p^0 = \frac{r_{12} + r_{23} \exp(2i q_{\perp 2} \Lambda)}{1 + r_{12} r_{23} \exp(2i q_{\perp 2} \Lambda)}, \quad (45)$$

$$t_p^0 = \frac{(1 - r_{12})(1 - r_{23})}{1 + r_{12} r_{23} \exp(2i q_{\perp 2} \Lambda)} \exp[i(q_{\perp 2} - q_{\perp 3})\Lambda], \quad (46)$$

and

$$\tilde{\beta}^{(m)} = \frac{\beta^{(m)}}{A_1}. \quad (47)$$

With the aid of Eqs. (43) and (44), we immediately find from Eq. (9) that the amplitude reflection (\tilde{r}_p) and transmission (\tilde{t}_p) coefficients of the MQW structure are given by

$$\tilde{r}_p \equiv -\frac{B_0}{A_0} = \frac{\tilde{T}_{22} r_p - \tilde{T}_{21}}{\tilde{T}_{11} - \tilde{T}_{12} r_p}, \quad (48)$$

$$\tilde{t}_p \equiv \frac{A_3}{A_0} = \frac{t_p}{\tilde{T}_{11} - \tilde{T}_{12} r_p}. \quad (49)$$

Note that, if there is no DBR between the prism and the barrier layer, $\tilde{\mathbf{T}} = \mathbf{U}$, and Eq. (48) is reduced to that given in Ref. 25.

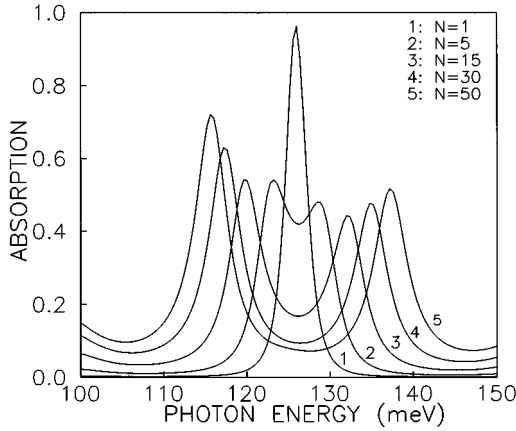


FIG. 1. Optical-absorption spectra of MQW's inside the microcavity for different QW numbers at a fixed cavity length of $\Lambda=2.978 \mu\text{m}$. The period number of the DBR is $N_m=5$.

If medium 3 is transparent [$\varepsilon_3(\omega)$ is real] and the total reflection condition is not reached for the barrier-medium 3 boundary ($q_{\perp 3}$ is real), it can be shown that the power transmission coefficient of the MQW structure is given by³⁴

$$T_p = \frac{q_{\perp 1} \varepsilon_3}{q_{\perp 3} \varepsilon_1} |\tilde{r}_p|^2. \quad (50)$$

The optical absorption coefficient of the MQW structure is then defined, from energy flux conservation, as

$$A_p = 1 - |\tilde{r}_p|^2 - T_p. \quad (51)$$

In this paper, however, we are interested in the case where light is totally reflected from the barrier-medium 3 interface in order to enhance the electromagnetic interaction among QW's, and therefore $T_p=0$.

III. NUMERICAL CALCULATIONS AND DISCUSSION

In this section we present various numerical calculations of the optical intersubband absorption spectra of a GaAs/Al_{0.33}Ga_{0.67}As MQW structure containing N identical QW's positioned between vacuum [$\varepsilon_3(\omega)=1.0$] and a GaAs/AlAs DBR followed by a GaAs prism. Experimentally, the prism can be realized by cleaving the side faces of the GaAs substrate. In our calculations the following material parameters, which are appropriate for this structure, were adopted. The barrier height is 256 meV, $m^*=0.067m_0$, $\varepsilon_2(\omega)\approx 10.0$, $\varepsilon_1(\omega)\approx 10.9$, and $\varepsilon_4(\omega)\approx 8.4$.³⁵ The static relative dielectric constant that enters the Poisson equation is $\varepsilon_r=13.0$. For each QW in the MQW structure, we assume that only the well layer is uniformly doped. The well and barrier widths in the MQW structure are taken to be 80 and 200 Å, respectively. The thicknesses of GaAs and AlAs layers forming the DBR are $L_1=1.289 \mu\text{m}$ and $L_4=2.342 \mu\text{m}$. Without special notification the sheet electron density is $N_s=1.2\times 10^{12} \text{ cm}^{-2}$, $\hbar/\tau=5.0 \text{ meV}$, and $\theta=55.0^\circ$. Note that, when the angle of incidence is larger than 17.6° , the light is totally reflected from the Al_{0.33}Ga_{0.67}As-vacuum interface for our structure under consideration. In addition, we assume in this paper that the MQW's are always placed in the middle

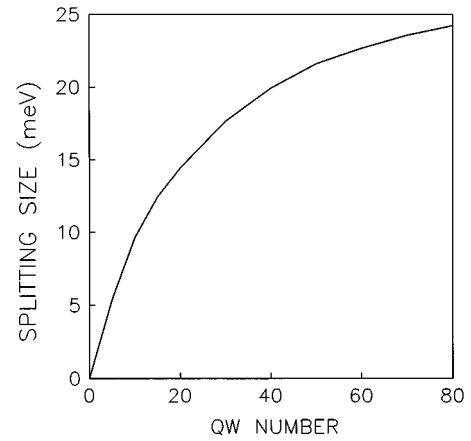


FIG. 2. The QW-number dependence of the Rabi splitting of the intersubband absorption spectra of a MQW structure. In the calculation, a cavity length of $\Lambda=2.978 \mu\text{m}$ was used. The period number was taken to be $N_m=5$.

of the cavity, i.e., $a=b$, although our theory is able to deal with other geometries.

In Fig. 1 we show the optical-absorption spectra of the MQW-embedded microcavity for different values of N and for a fixed effective cavity length of $\Lambda=2.978 \mu\text{m}$. In all calculations the period number of the DBR is $N_m=5$. It appears from Fig. 1 that, when a single QW ($N=1$) is placed inside the microcavity, the absorption spectrum of the structure has only one absorption peak in the frequency range used in Fig. 1. This peak corresponds to the local-field-shifted intersubband resonance.^{11,15} In this case, the coupling between the intersubband mode and the cavity mode is insufficiently strong, resulting in a noticeable splitting of the absorption spectrum because a finite relaxation time of electrons was taken into account in our calculations. At this point, we would like to remind the reader that, if the line-broadening effect and the conduction-band nonparabolicity are neglected, the splitting of the intersubband mode and the cavity mode should always exist.²⁴ We have also checked that, in the case where the electron relaxation time tends to

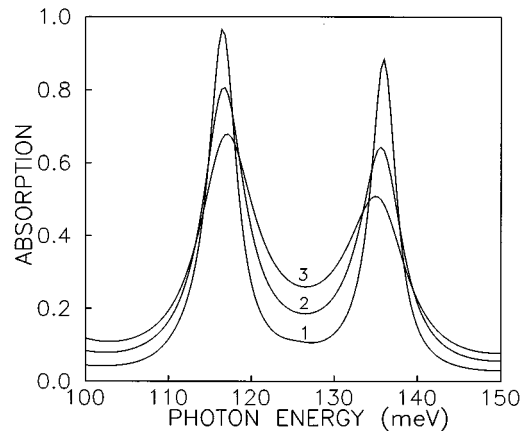


FIG. 3. Optical-absorption spectra of a MQW structure having 35 QW's for different values of the relaxation time, i.e., $\hbar/\tau=3.0$ (curve 1), 6.0 (curve 2), and 9.0 meV (curve 3). The cavity length is $\Lambda=2.978 \mu\text{m}$, and the period number is $N_m=4$.

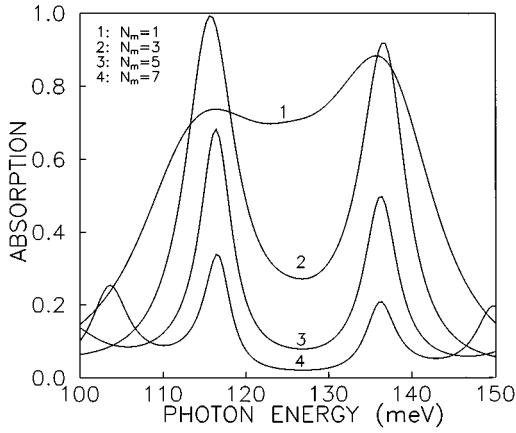


FIG. 4. Optical-absorption spectra of a MQW structure having 40 QW's for different values of the period number N_m . The cavity length is $\Lambda=2.978 \mu\text{m}$.

infinity and the band nonparabolicity effect is included, the splitting exists as well. This result may be due to the fact that the local-field (depolarization) effect strongly compensates the nonparabolicity-induced line broadening.³⁶ It in turn implies that the nonparabolic dispersion of the electronic subbands *does not* significantly affect the splitting of the intersubband absorption spectrum. When more QW's are included in the cavity, one can see clearly from Fig. 1 that an obvious splitting of the spectrum occurs (see curves 2–5 for $N \geq 5$). This result suggests that, only when the effective oscillator strength of the MQW structure that is essentially proportional to the number of QW's is large enough, the Rabi splitting of the intersubband absorption line can happen. One can also see from Fig. 1 that, as the QW number is increased, the size of the splitting is substantially increased. A detailed graphic illustration of the QW-number dependence of the Rabi splitting is given in Fig. 2. Note that all parameters used in Fig. 2 are identical to those in Fig. 1. It appears from Fig. 2 that the size of the Rabi splitting increases roughly in proportion to the square root of the well number, as has been recently shown for the Rabi splitting of

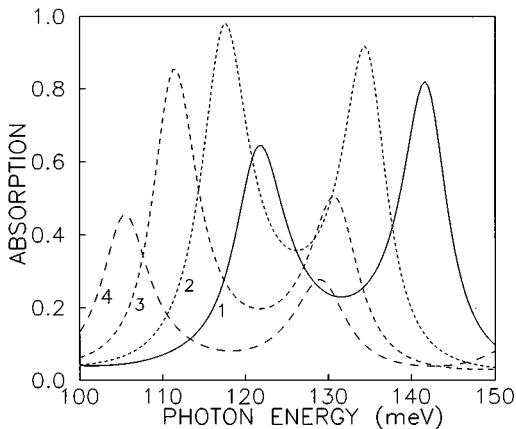


FIG. 5. Optical-absorption spectra of a MQW structure having 25 QW's for different values of the cavity length, i.e., $\Lambda=2.383$ (curve 1), 2.978 (curve 2), 3.574 (curve 3), and $4.170 \mu\text{m}$ (curve 4). The period number is $N_m=3$.

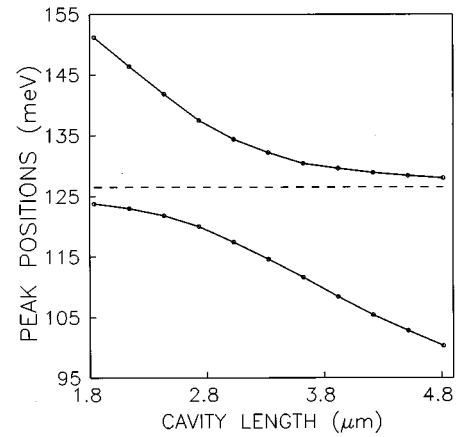


FIG. 6. The peak positions of the Rabi-split absorption spectrum as a function of the cavity length. In the calculation we have chosen $N=25$ and $N_m=3$. The local-field-shifted resonance energy of the free-standing QW's is indicated by the dashed line.

the exciton-polariton branches by Ivchenko *et al.*³⁷ In addition, we also note from Fig. 1 that the contrast of the Rabi splitting that is characterized by the ratio between the heights of the peak and the bottom in the spectrum becomes bigger when N is larger.

In order to see the influence of the relaxation time on the Rabi splitting of the absorption spectra, we have calculated the optical spectra for different values of \hbar/τ , namely, $\hbar/\tau=3.0, 6.0$, and 9.0 meV . The calculated results for $N=35$, and $N_m=4$ are presented in Fig. 3. The cavity length used in this figure is the same as in Fig. 1. From Fig. 3 one sees that, as τ is increased, the separation between the two main peaks is slightly increased. As one would expect, however, the contrast of the Rabi splitting becomes better when \hbar/τ is smaller.

We now investigate the effect of the period number N_m on the Rabi splitting of the absorption spectra of the MQW's. Because the optical reflection coefficient of the DBR strongly depends on the value of N_m ,³² one can expect that the variation of N_m leads to a large modification of the ab-

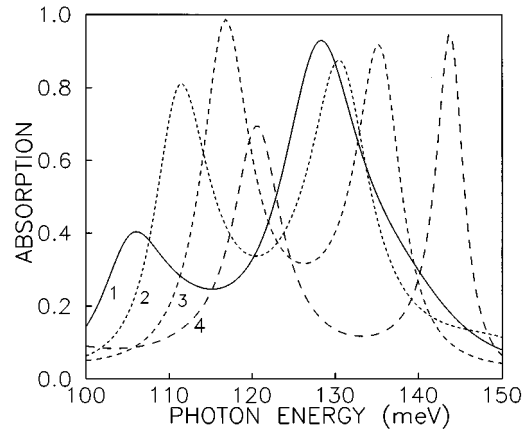


FIG. 7. Optical-absorption spectra of a MQW structure have 30 QW's for different values of the angle of incidence, i.e., $\theta=51.0^\circ$ (curve 1), 53.0° (curve 2), 55.0° (curve 3), and 57.0° (curve 4). The period number of the DBR is $N_m=3$, and the cavity length is $\Lambda=2.978 \mu\text{m}$.

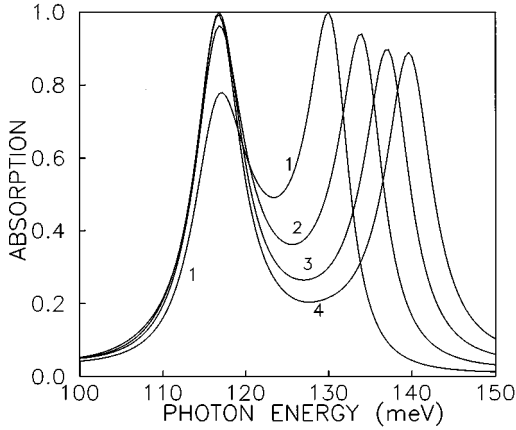


FIG. 8. Optical-absorption spectra of a MQW structure having 30 QW's for different values of the sheet electron concentration (in units of 10^{12} cm^{-2}), i.e., $N_s=0.5$ (curve 1), 1.0 (curve 2), 1.5 (curve 3), and 2.0 (curve 4). The period number of the DBR is $N_m=3$, and the cavity length is $\Lambda=2.978 \mu\text{m}$.

sorption spectrum. This is illustrated in Fig. 4. In this figure we show the absorption spectra of the MQW's with $N=40$ for different values of N_m . Again, a cavity length of $\Lambda=2.978 \mu\text{m}$ was used in the calculations. We can clearly see from Fig. 3 that N_m has a large influence on the magnitude of the absorption coefficient as well as on the contrast of the Rabi splitting. However, it seems that the size of the splitting is only slightly dependent of the period N_m . One also notes from Fig. 3 that, when the number of the period is large ($N_m=7$), more absorption peaks appear in the spectrum. This result stems from the multiple reflection (interference effect) of the light among the multilayers inside the DBR.³²

Since the cavity resonance frequency is strongly dependent of the cavity length and the angle of incidence, it is expected that the Rabi splitting can be tuned by varying either the cavity length or the angle of incidence in an appropriate range. (To avoid the appearance of a new cavity mode interacting with the intersubband mode, the cavity length and the angle of incidence should not be changed too much.) In Fig. 5 we show the optical-absorption spectra of our MQW structure for different cavity lengths, ranging from $\Lambda=2.383$ to $4.170 \mu\text{m}$. In the calculations $N=25$ and $N_m=3$ were employed. By a view of Fig. 5 one clearly sees that, as the cavity length is changed, the positions of the two peaks in the optical spectra are also varied. A summary of this change is shown in Fig. 6. In this figure we display the peak positions of the coupled cavity-quantum-well modes (solid lines with points) as a function of the cavity length. For reference, the intersubband resonance energy of the free-standing MQW's is also indicated in Fig. 6 by the dashed line. From Fig. 6 one can clearly observe the characteristic anticrossing splitting. Returning to Fig. 5, one notices that the absorption line shape and the peak value are also strongly dependent on the cavity length. This suggests that to characterize fully the photon-mode-intersubband-excitation coupling, it is in general necessary to analyze the absorption line shape in addition to the peak positions.

In Fig. 7 are shown the optical-absorption spectra of the MQW structure as a function of the angle of incidence. In the

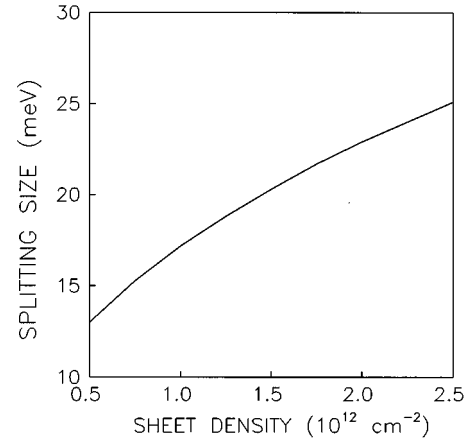


FIG. 9. The size of the Rabi splitting as a function of the sheet electron density. The QW number is $N=30$, the period number of the DBR is $N_m=3$, and the cavity length is $\Lambda=2.978 \mu\text{m}$.

calculations $N=30$, $N_m=3$, and $\Lambda=2.978 \mu\text{m}$ were used. As in Fig. 5, we see from Fig. 7 that varying the angle of incidence also leads to an obvious change in the size of the splitting and in the absorption spectrum.

Finally, let us discuss the influence of the sheet electron concentration on the Rabi splitting of the absorption spectrum. To this end, we have calculated the absorption spectra of the MQW's for different values of N_s ranging from 0.5 to $2.5 \times 10^{12} \text{ cm}^{-2}$. The other parameters employed in our calculations are $N=30$, $N_m=3$, and $\Lambda=2.978 \mu\text{m}$. Some of the calculated absorption spectra are presented in Fig. 8. It is interesting to notice from Fig. 8 that, with an increase in the sheet electron density, the higher-energy peak is shifted upwards, whereas the lower-energy peak almost does not move. This result should be expected, since the local-field-shifted intersubband resonance energy of the free-standing QW's is shifted upward with increasing N_s ,¹¹ whereas the cavity resonance energy does not change. As a consequence, only the higher-energy peak is noticeably shifted. In turn, the size of the Rabi splitting increases with increasing the electron density. This electron concentration dependence of the peak separation is shown in Fig. 9. Also, one can see from Fig. 8 that the contrast of the splitting is strongly dependent of N_s . The larger the sheet electron density is, the better the contrast is. This indicates that a heavily doped MQW structure is more favorable to observe a large Rabi splitting.

IV. CONCLUSION

Using a combined transfer-matrix and Green's-function formalism in which nonlocal effects in the optical intersubband response of the MQW system and the conduction band nonparabolicity effect are taken into account, we have derived a rigorous expression for the intersubband optical absorption coefficient of a MQW structure inside an asymmetric Fabry-Pérot microcavity that is formed from a DBR and a light-total-reflection dielectric interface. As a numerical example, we calculated the optical-absorption spectra of a GaAs/ $\text{Al}_{0.33}\text{Ga}_{0.67}\text{As}$ MQW structure positioned between vacuum and a GaAs/AlAs DBR. To enhance the intersubband interactions of our MQW system, we considered the

case where the incident light is coupled into the MQW structure from a GaAs prism. In numerical calculations, we paid special attention to the influence of various cavity and QW material parameters on the Rabi splitting of the intersubband absorption spectrum in the strong-coupling regime. Our calculations show that, with an increase in the QW number and in the electron concentrations, the size of the Rabi splitting is

increased, and the contrast of the splitting becomes better as well. In addition, it has been shown that varying the period number N_m of the DBR results in a large modification of the contrast of the Rabi splitting. However, the size of the splitting is only slightly dependent on N_m . Finally, we demonstrated that the Rabi splitting can be easily tuned by varying either the cavity length or the angle of incidence.

-
- ¹L. C. West and S. J. Eglash, *Appl. Phys. Lett.* **46**, 1156 (1985).
²A. Harwit and J. S. Harris, Jr., *Appl. Phys. Lett.* **50**, 685 (1987).
³B. C. Covington, C. C. Lee, B. H. Hu, H. F. Taylor, and D. C. Streit, *Appl. Phys. Lett.* **54**, 2145 (1989).
⁴M. Ramsteiner, J. D. Ralston, P. Koidl, B. Dischler, H. Beibl, J. Wagner, and H. Ennen, *J. Appl. Phys.* **67**, 3900 (1990).
⁵M. O. Manasreh, F. Szmulowicz, T. Vaughan, K. R. Evans, C. E. Stutz, and D. W. Fischer, *Phys. Rev. B* **43**, 9996 (1991).
⁶B. Jagai, M. O. Manasreh, C. E. Stutz, R. L. Whitney, and D. K. Kinell, *Phys. Rev. B* **46**, 7208 (1992).
⁷M. S.-C. Luo, S. L. Chuang, S. Schmitt-Rink, and A. Pinzuk, *Phys. Rev. B* **48**, 11 086 (1993).
⁸J. N. Heyman, K. Craig, B. Galdrikian, M. S. Sherwin, K. Campman, P. F. Hopkins, S. Fafard, and A. C. Gossard, *Phys. Rev. Lett.* **72**, 2183 (1994).
⁹G. Gumbs, D. Huang, and J. P. Loehr, *Phys. Rev. B* **51**, 4321 (1995).
¹⁰D. Huang, G. Gumbs, and M. O. Manasreh, *Phys. Rev. B* **52**, 14 126 (1995).
¹¹A. Liu, *Phys. Rev. B* **50**, 8569 (1994).
¹²T. Stroucken, A. Knorr, C. Anthony, A. Schulze, P. Thomas, S. W. Koch, M. Koch, S. T. Cundiff, J. Feldmann, and E. O. Göbel, *Phys. Rev. Lett.* **74**, 2391 (1995).
¹³T. Stroucken, C. Anthony, A. Knorr, P. Thomas, and S. W. Koch, *Phys. Status Solidi B* **188**, 539 (1995).
¹⁴T. Stroucken, A. Knorr, P. Thomas, and S. W. Koch, *Phys. Rev. B* **53**, 2026 (1996).
¹⁵A. Liu, *Phys. Rev. B* (to be published).
¹⁶Y. Yamamoto, S. Machida, and G. Björk, *Phys. Rev. A* **44**, 657 (1991).
¹⁷C. Weisbuch, M. Nishioka, A. Ishikawa, and Y. Arakawa, *Phys. Rev. Lett.* **69**, 3314 (1992).
¹⁸D. S. Citrin, *IEEE J. Quantum Electron.* **30**, 997 (1994).
¹⁹R. Houdré, C. Weisbuch, R. P. Stanley, U. Oesterle, P. Pellandini, and M. Ilgms, *Phys. Rev. Lett.* **73**, 2043 (1994).
²⁰P. Kelkar, V. Kozlov, H. Jeon, A. V. Nurmikko, C.-C. Chu, D. C. Grillo, J. Han, C. G. Hua, and R. L. Gunshor, *Phys. Rev. B* **52**, R5491 (1995).
²¹G. Panzarini and L. C. Andreani, *Phys. Rev. B* **52**, 10 780 (1995).
²²R. P. Stanley, R. Houdré, C. Weisbuch, U. Oesterle, and M. Ilgms, *Phys. Rev. B* **53**, 10 995 (1996).
²³T. A. Fisher, A. M. Afshar, M. S. Skolnick, D. M. Whittaker, and J. S. Roberts, *Phys. Rev. B* **53**, R10469 (1996).
²⁴D. A. Dahl and L. J. Sham, *Phys. Rev. B* **16**, 651 (1977).
²⁵A. Liu, *J. Appl. Phys.* **80**, 1928 (1996).
²⁶L. Wendler and E. Kändler, *Phys. Status Solidi B* **177**, 9 (1993).
²⁷A. Bagchi, *Phys. Rev. B* **15**, 3060 (1977).
²⁸P. J. Feibelman, *Prog. Surf. Sci.* **12**, 287 (1982).
²⁹For simplicity, we have assumed the effective mass of electrons that enters the interaction Hamiltonian is the same even when the electrons penetrate the barrier layers. In addition, the conduction-band nonparabolicity effect is only included in the light-unperturbed Hamiltonian (see Refs. 30 and 31).
³⁰U. Ekenberg, *Phys. Rev. B* **40**, 7714 (1989).
³¹See, for example, M. E. Lazzouni and L. J. Sham, *Phys. Rev. B* **48**, 8948 (1993).
³²P. Yeh, A. Yariv, and C.-S. Hong, *J. Opt. Soc. Am.* **67**, 423 (1977).
³³J. E. Sipe, *J. Opt. Soc. Am. B* **4**, 481 (1987), and references therein.
³⁴J. A. Kong, *Electromagnetic Wave Theory* (Wiley, New York, 1986).
³⁵J. P. van der Ziel and A. C. Gossard, *J. Appl. Phys.* **49**, 2919 (1978).
³⁶M. Zaluzny, *Phys. Rev. B* **43**, 4511 (1991).
³⁷E. L. Ivchenko, M. A. Kaliteevski, A. V. Kavokin, and A. I. Nesvikhskii, *J. Opt. Soc. Am. B* **13**, 1061 (1996).